

Biomolecular dynamics studied with IR-spectroscopy using quantum cascade lasers combined with nanosecond perturbation techniques

Alexander Popp¹, David Scheerer¹, Benjamin Heck, Karin Hauser*

Department of Chemistry, University of Konstanz, 78457 Konstanz, Germany

A B S T R A C T

Early events of protein folding can be studied with fast perturbation techniques triggering non-equilibrium relaxation dynamics. A nanosecond laser-excited pH-jump or temperature-jump (T-jump) was applied to initiate helix folding or unfolding of poly-L-glutamic acid (PGA). PGA is a homopolymer with titratable carboxyl side-chains whose protonation degree determines the PGA conformation. A pH-jump was realized by the photochemical release of protons and induces PGA folding due to protonation of the side-chains. Otherwise, the helical conformation can be unfolded by a T-jump. We operated under conditions where PGA does not aggregate and temperature and pH are the regulatory properties of its conformation. The experiments were performed in such a manner that the folding/unfolding jump proceeded to the same PGA conformation. We quantified the increase/decrease in helicity induced by the pH-/T-jump and demonstrated that the T-jump results in a relatively small change in helical content in contrast to the pH-jump. This is caused by the strong pH-dependence of the PGA conformation. The conformational changes were detected by time-resolved single wavelength IR-spectroscopy using quantum cascade lasers (QCL). We could independently observe the kinetics for α -helix folding and unfolding in PGA by using different perturbation techniques and demonstrate the high sensitivity of time-resolved IR-spectroscopy to study protein folding mechanisms.

Keywords:

T-jump
pH-Jump
Infrared spectroscopy
Quantum cascade laser
Folding kinetics
Poly-L-glutamic acid

1. Introduction

Understanding the molecular mechanisms of protein folding is of fundamental importance since misfolded proteins can lose their function or even cause diseases. Much of our knowledge has been derived from *in vitro* studies revealing that protein folding involves several structural transitions including backbone ordering, hydrogen bond formation and side-chains packing. These fundamental processes are difficult to observe with equilibrium measurements and are better analyzed with perturbation techniques. Infrared (IR) spectroscopy is well established to investigate secondary structure formation and to gain insights into the molecular mechanisms of protein folding on all relevant time-scales. In order to observe early events in protein folding, sub-millisecond time-resolution and fast triggering methods are required. Pulsed laser-excitation can be used to generate fast jumps in temperature or in pH and to study relaxation dynamics of peptides and proteins [1,2].

We built-up a quantum cascade laser based IR-spectrometer combined with a laser-excited temperature-jump (T-jump) or alternatively with a pH-jump for the fast (nanosecond) initiation of non-equilibrium

protein folding dynamics. The T-jump was induced by a Q-switched Ho:YAG laser pulse exciting the frequency of an overtone vibration of the solvent D₂O. The change in water absorbance acts as an internal thermometer and is used to determine the magnitude of the T-jump spectroscopically. The perturbation in a T-jump experiment is often small resulting in a transition of overlapping ensembles of states. However, even if the induced conformational dynamics might be minor, T-jump studies can provide insights into protein folding mechanisms as we and others have shown. For example, we have probed differences in relaxation dynamics on the basis of individual amino acids using site-specific labeling or mutations [3,4]. A larger perturbation might be induced by a pH-jump if titratable amino acid side-chains have a significant impact on the protein conformation. The pH-jump was induced photochemically by UV photolysis of *o*-nitrobenzaldehyde (*o*NBA) resulting in the formation of an *o*-nitrosobenzoic acid product, the release of protons and a persistent reduction of the pH [5–8]. The photoreaction of *o*NBA has been characterized in detail [6] and is not infinitely fast, but the proton release occurs after a few tens of nanoseconds which limits the time-resolution of the pH-jump experiment. The UV pulse was produced by a Q-switched Nd:YAG laser equipped with a fourth harmonic generator. Since all experiments were performed in D₂O, a “pD-jump” rather than a “pH-jump” was applied. However, we use the expression “pH-jump” when we refer to our triggering method in order to be consistent

* Corresponding author.

E-mail address: karin.hauser@uni-konstanz.de (K. Hauser).

¹ These authors contributed equally.

with the literature. IR folding studies commonly use the amide I band for secondary structure analysis (mainly C=O stretching vibration of the polypeptide backbone) and are performed with the solvent D₂O instead of H₂O since the strong absorbance of the OH bending vibration overlays the amide I region (1700 cm⁻¹–1600 cm⁻¹). Due to the isotope effect, the OD bending vibration is frequency-shifted to lower wavenumbers and the amide I band is called amide I'. In our spectrometer setup we use a quantum cascade laser (QCL) as IR source. The QCL is tunable over the whole amide I' region and conformational dynamics can be probed after perturbation at various single wavelengths.

Poly-L-glutamic acid (PGA) is a homopolypeptide with solely titratable side-chains and an ideal model peptide to study helix formation. At neutral pH, disordered (coil) conformation is favored due to the electrostatic Coulomb repulsion of the ionized side chains. At acidic pH, more side-chains of PGA are protonated and the fraction of helical conformation increases. The conformation respectively the free energy of PGA depends on several factors, e.g. concentration, temperature, the ionic strength of the solvent and the number of titratable groups (chain length). Several T-jump [9–11] and pH-jump [5,7] measurements on PGA have been carried out recently. These and other studies [12–17] analyzed the stability and folding mechanism of PGA including helix nucleation, H-bond formation and helix propagation. The methods and measurement conditions differ among the studies and thus the conclusions about folding mechanisms are sometimes difficult to compare.

In this study, we compare the relaxation dynamics of PGA after a T-jump and after a pH-jump. The T-jump shifts the new equilibrium to a conformation with less helical content upon thermal unfolding and at a constant pD. In the pH-jump experiment, the released protons neutralize the carboxylate groups of the side-chains of the peptide that in turn folds into an α -helix due to the diminished repulsive charges. Conformational dynamics were induced at a constant temperature towards an increased helical content. The starting conditions of both experiments were different, i.e. the initial temperature T_i in the T-jump experiment ($pD_f, T_i \rightarrow T_f$) and the initial pD_i in the pH-jump experiment ($T_f, pD_i \rightarrow pD_f$), but the magnitudes of the jumps were adjusted to proceed to the same final conditions (pD_f, T_f). Thus, presumably the same final conformation was adopted by PGA after perturbation to the new equilibrium in both experiments as illustrated schematically in Fig. 1. We measured the relaxation times for the pH-induced folding and the temperature-induced unfolding towards equal PGA helicity and evaluated if there are mechanistic differences or similarities. Both, T-jump and pH-

jump methods have been applied to PGA previously, however never in combination with each other.

2. Experimental section

2.1. Sample preparation for IR measurements

Poly-L-glutamic acid sodium salt (PGA) with an average degree of polymerization of 136 residues was obtained from Sigma-Aldrich and used without further purification. All IR experiments were performed in D₂O as solvent using CaF₂ cells with a path length of 100 μ m. The pH values were measured by a calibrated glass electrode (BIOTRODE, Metrohm AG, Switzerland) and corrected by 0.4 in order to obtain the corresponding pD value [18]. For pH jump experiments, PGA was dissolved at a concentration of 2 mg/mL in a saturated solution of oNBA in D₂O. Accordingly, the concentration of the protonatable glutamic acid side chains amounts to 13 mM. Before addition of PGA, the oNBA solution was filtered and the final oNBA concentration was measured by the absorbance at $\lambda = 266$ nm leading to a value of $c = 8$ mM (using an extinction coefficient ϵ of 8300 M⁻¹ cm⁻¹ [5]). An initial pD of 6 was adjusted by adding 0.1 M DCl to the PGA/oNBA/D₂O solution. For T-jump measurements, a PGA concentration of $c = 20$ mg/mL in D₂O was prepared. As the sample has a basic pD directly after dissolving, addition of 0.1 M DCl was necessary to obtain the desired pD value of 5.8. In order to reach the same (pH- and temperature-dependent) PGA conformation with both perturbation techniques, the final temperature (T_f) and pD value (pD_f) were chosen to be nearly identical, i.e. $T_f = 25.6$ °C at pD 5.8 after the T-jump and $pD_f 5.8$ at $T = 24.9$ °C after the pH-jump.

2.2. CD measurements

CD measurements were carried out with a J815 spectrometer (JASCO). Data were recorded between 300 nm and 180 nm with a scanning speed of 200 nm/min and a digital integration time of 0.25 s. The spectral resolution was 1 nm. Final spectra were averaged out of five scans, smoothed and a D₂O background spectrum was subtracted. The temperature was controlled by a regulated flow from a water bath (FL300, Julabo) through the cell holder. The measurements were carried out in Quartz cells (Starna) with 1 mm path length and at a concentration of 0.5 mg/mL. To adjust the desired pD value, deuterated sulfuric acid (D₂SO₄) was used instead of DCl due to the strong absorbance of chloride ions at low wavelengths. According to Rohl et al. [15], the

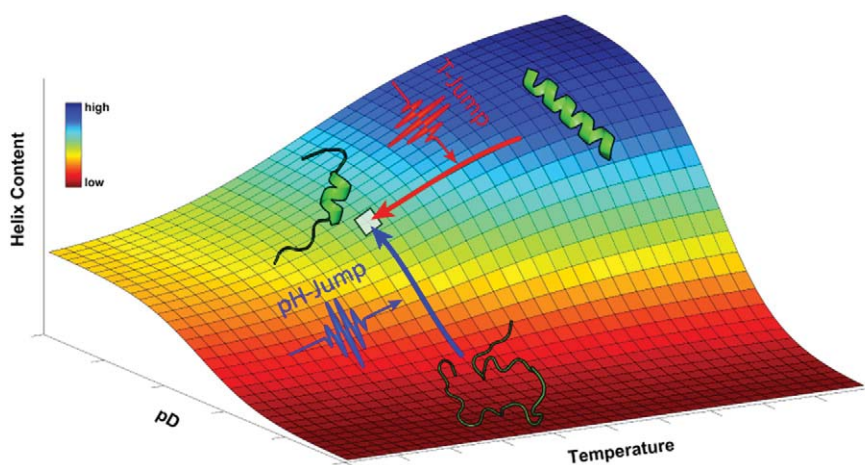


Fig. 1. Scheme illustrating the change in helicity of poly-L-glutamic acid (PGA) in dependence of temperature and pD. Nanosecond perturbation techniques, a laser-excited T-jump or pH-jump, were applied to study relaxation dynamics. A pH-jump initiates α -helix folding whereas a T-jump induces unfolding of PGA. The parameters were chosen in that manner that both perturbation experiments proceed to the same final conformation.

ellipticity recorded at 222 nm, θ_{222} , is assumed to be linearly related to the mean helix content f_H . The conversion of θ_{222} to f_H requires the knowledge of the base line ellipticities for the disordered (coil) conformation, θ_C , and for θ_H , assumed for a completely folded α -helix,

$$f_H = (\theta_{222} - \theta_C) / (\theta_H - \theta_C) \quad (1)$$

θ_C and θ_H are dependent on temperature and are given by the following expressions [19]:

$$\theta_C = 2220 - 53 T \quad (2)$$

$$\theta_H = (-44000 + 250T)(1 - 3/N_r) \quad (3)$$

where T is the temperature in $^{\circ}\text{C}$ and N_r is the chain length in residues. The helix content f_H was set to zero when θ_{222} values become positive and indicate a complete disordered conformation. Errors which were mostly caused by uncertainties in the amount of added acid are estimated to be in the range $\pm 4\%$ helix content for the pH-jump measurements.

2.3. Time-resolved IR measurements using a quantum cascade laser spectrometer

The quantum cascade laser (QCL) spectrometer was described in detail previously [20] and the current setup is shown in Fig. 2. Briefly, the mid-IR single wavelength emission of the QCL (Daylight Solutions Inc., U.S.A.) is used as cw probe source to monitor the relaxation dynamics. The tunable range lies between 1715 cm^{-1} and 1580 cm^{-1} and covers the whole amide I' region. The QCL beam (Fig. 2, red beam line) is focused to a diameter of $\sim 300\ \mu\text{m}$ at the center of the excited volume. A photovoltaic HgCdTe detector (18 MHz, KMPV11-1-J2, Kolmar Technologies, U.S.A.) was used to measure the transient changes in

transmission. The signals were digitized and recorded by a transient recorder board with 16 bit resolution (Spectrum, Germany).

2.3.1. Laser-excited T-jump

Some modifications related to the T-jump excitation were made recently in our spectrometer setup described in [20]. The previously used combination of a Nd:YAG laser and a Raman-shifter was replaced by a Q-switched Ho:YAG laser (IPG Photonics Corporation, U.S.A.) with an emission wavelength of 2090 nm. The Ho:YAG laser pulses excite directly (without need of Raman-shifting) an overtone vibration of D_2O leading to a rapid temperature jump within the excited volume. The pulse duration is 9 ns and the maximum pulse energy $E = 14\ \text{mJ}$ at 10 Hz repetition rate. A chopper was synchronized with the pump laser for acquisition of reference signals without pump light resulting in a repetition rate of 5 Hz for the excitation of the sample. The spot size of the beam was adjusted by the use of lenses and dichroic mirrors to heat an area of about 2 mm in diameter in the center of the sample cell. To enable a homogeneous heating of the sample volume, the pump pulse is split by a 50:50 beam splitter into two counter-propagating beams. Different neutral density attenuators were used in order to adjust the magnitude of the temperature jump, in this study to $\Delta T = 6.6\ ^{\circ}\text{C}$. The final temperature was calculated at the respective wavenumber used for the T-jump measurement by referencing the temperature change to temperature-dependent FTIR spectra of the solvent D_2O . The final temperature of the excited volume was $25.6\ ^{\circ}\text{C}$. The pD of the peptide sample was set to 5.8, corresponding to the final pD value in the pH-jump experiments.

2.3.2. Laser-excited pH-jump

A 5 ns UV light pump pulse at 266 nm is produced by a Q-switched Nd:YAG laser equipped with a fourth harmonic generator as described previously [20]. The pulse energy $E = 85\ \mu\text{J}$ and spot size $\sim 1\ \text{mm}$ in diameter were adjusted by neutral density attenuators and a UV focusing

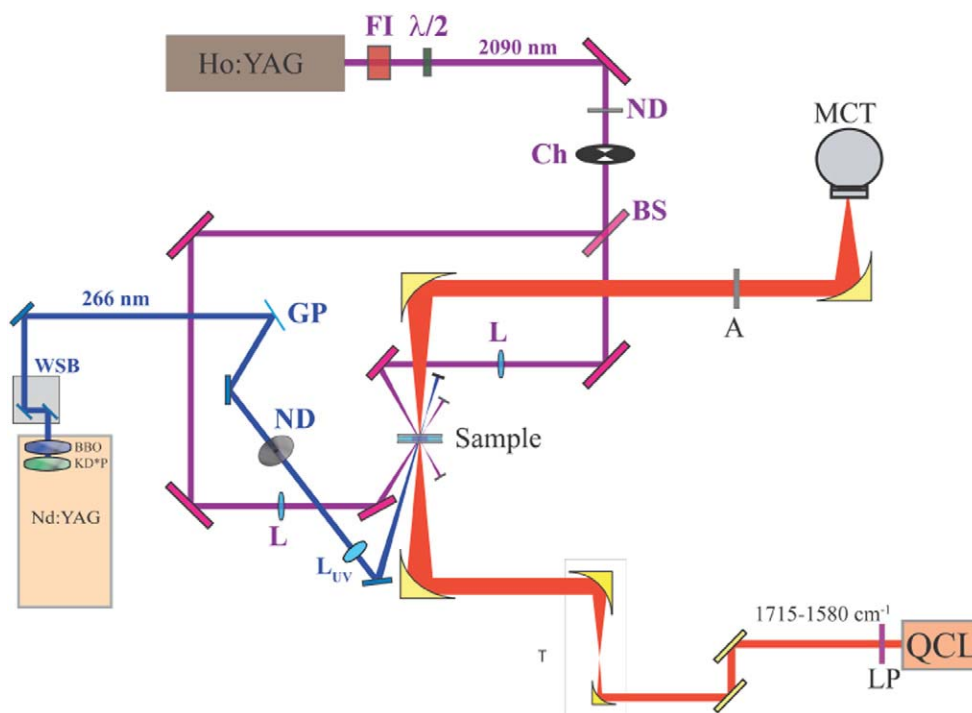


Fig. 2. Scheme of the quantum cascade laser spectrometer combined with laser-excited perturbation techniques. A quantum cascade laser is used to monitor the relaxation kinetics (red beam line) initiated by a T-jump (excitation at 2090 nm, purple beam line) or by a photochemically induced pH-jump (excitation at 266 nm, blue beam line). QCL: quantum cascade laser tunable between 1715 and 1580 cm^{-1} (IR probe laser); LP: long pass filter; T: telescope; A: attenuator; MCT: photovoltaic HgCdTe detector; Ho:YAG: Q-switched Ho:YAG laser (pump pulse for the T-jump); FI: Faraday isolator; $\lambda/2$: $\lambda/2$ plate; ND: neutral density attenuator; Ch: chopper; BS: beamsplitter; L: focusing lenses for the pump pulse at 2090 nm; Nd:YAG: Q-switched Nd:YAG laser (pump pulse for the pH-jump); BBO, KD*P: non-linear crystals for fourth harmonic generation; WSB: wavelength separation box; GP: glass plate; ND: neutral density attenuator; L_{UV} : focusing lens for the 266 nm pump pulse.

lens to ensure an appropriate proton release from oNBA to initiate the folding of PGA, but also to prevent distortions and damage of the IR cell. As the pH-jump experiment was performed in a non-reversible manner, the sample was placed in a flow-through IR cell. In this experiment the repetition rate of the pump laser was set to 10 Hz. The sample was pumped through the cell by use of a peristaltic pump and the pumping velocity was adjusted in the way that the bleached volume was removed from the probed volume just before the next excitation pulse. The excited volume remained undisplaced for at least 1 ms as long as the relaxation kinetics were monitored. A small temperature jump of ~ 1 °C was identified in the recorded transients caused by the heating of the 266 nm excitation pulses. It was monitored by a negative change in the transient absorbance spectra ΔA directly after the excitation pulse. This absorbance change is attributed to the change in the sample temperature and it was quantified by reference measurements of oNBA in D₂O in the absence of PGA. Accordingly, the final sample temperature for the pH-jump measurements including this heating was $T = 24.9$ °C. The pH-jump was estimated indirectly by calculating the number of released protons into the solution. One laser pulse consists of $n_{\text{ph}} = 1.14 \cdot 10^{14}$ photons. Due to the quantum yield of the photon absorption and proton release by oNBA, the number of released protons is $\frac{1}{4} n_{\text{ph}} = 2.85 \cdot 10^{13}$ [5,7,21]. As the number of protonatable side chains of PGA in the excited volume is $6.4 \cdot 10^{14}$ ($c = 2$ mg/mL and $V_{\text{ex}} = 0.0785$ μL) only a small part of the side chains, 4.5%, is additionally protonated. From this change in protonation, the corresponding pH-jump can be calculated. For the initial pD of 6.0 and using Table 1, the final pD_f after the pH-jump was determined to be 5.8.

2.3.3. Data evaluation

In both experiments, pH-jump and T-jump, the solvent and peptide sample were measured separately in a refillable IR cell. This has the advantage of highly reproducible measurement conditions, e.g. the path length and the positioning of the IR cell in respect to the overlap adjustment of the pump and probe beams in the excited sample volume, what leads to a more reliable subtraction of the solvent from the peptide kinetics. Several thousands of transients were collected and processed using an in-house developed software filter (Matlab software) to increase the data quality by discarding those transients distorted by cavitation. About 900 transients for the T-jump and 1200 transients for the pH-jump were averaged. The solvent signal subtraction is an important step which has to be performed carefully. As PGA does not show any millisecond kinetics its transient signal reaches a final value in this time region. The solvent signal (~ 1000 transients, for both T-jump and pH-jump) was scaled appropriately and subtracted from the peptide/solvent mixture signal. The solvent-corrected transients were further subjected to averaging, so that an equal number of points (20 points per decade) were distributed in each time decade. This quasi-

logarithmic averaging procedure leads to a significant reduction of noise and signal distortions (Fig. 3). Furthermore, the weighting of the data points in every decade is evenly distributed and the data points at early time scale are not underrepresented in the fit procedure, as it is often the case with linear data recording. The method ensures a more reliable data fitting of transient spectra on a logarithmic time scale. After evaluation of several fit functions, the transients of PGA at 1630 cm^{-1} were fitted by a bi-exponential function

$$\Delta A = A_0 + A_1 e^{-\frac{t}{\tau_1}} + A_2 e^{-\frac{t}{\tau_2}} \quad (4)$$

and in the time interval between 340 ns and 1 ms.

3. Results and discussion

3.1. Helical content in dependence of temperature and pH

CD measurements of PGA have been performed in dependence of temperature (at a pD of 5.8) as well as in dependence of pD (at $T = 25$ °C) in order to determine the helical content. The titration data for PGA are the cornerstone for the design of the kinetic pH-jump experiments since they provide the correlation between pD, side chain protonation and helicity of PGA. Accordingly, an exactly known amount of PGA was titrated with D₂SO₄. The pD was measured as a function of the added titrant starting from pD 8.3 down to pD 4.1. No additional buffers were present in the solution, therefore a 1:1 neutralization reaction between D₂SO₄ and PGA was assumed neglecting the minimal presence of hydroxyl groups at the initial pD and of free protons at pD 4.1.

Table 1 depicts the helical content of PGA (f_{H}) in dependence of the degree of protonation at a temperature of 25 °C. The helix content was determined by the CD signal at 222 nm as described in the Experimental section and f_{H} was set to zero for positive values of θ_{222} which indicate a complete disordered conformation [15]. A threshold of about 40% protonation was observed before folding starts. Above 80% protonation, the peptide adopts an almost complete helical structure. However, the strongly protonated PGA molecules also tend to aggregate due to the loss of the electrostatic repulsion. Aggregation is indicated for pD 4.1 since the continuous decrease in band intensity at 222 nm upon lowering the pH is interrupted and the intensity increases again between pD 4.8 and 4.1 (Table 1). In addition, at pD 4.1, the relative intensity of the band at 222 nm is increased in comparison to the band at 208 nm in contrast to all other pD values (data not shown) what was interpreted as evidence for aggregation [22]. Thus the data point at pD 4.1 was disregarded for the fit in the helix content (Fig. 4, blue curve). The sigmoidal shape of the curve was described by a Boltzmann function with an inflection point at 66% protonation what corresponds to a pD of 6.1. The initial pD was chosen to be close to the inflection point and set to 6.0 in the pH-jump experiment. As pointed out in the Experimental Section 2.3.2, the pH-jump increases the protonation of the side chains of about 4.5%. This change in protonation leads to an increase in helix content from 60% to 80%. With the quantification of 20% helicity change, the magnitude of the pH-jump can be derived from the calibration curve. A pH-jump of $\Delta\text{pD} = -0.2$ was determined leading to the final value pD_f 5.8. For comparison with the T-jump experiment, thermal unfolding of PGA at pD_f 5.8 was also monitored (Fig. 4, red curve). Due to the repulsion of negatively charged glutamate groups at pD 5.8, PGA is not completely helical even at low temperatures about 5 °C. The helix content decreases from 90% to 31% with increasing temperature. The thermal unfolding transition is much broader than the pH induced folding transition under the chosen conditions. Therefore, a T-jump of 6.6 °C from $T_i = 19$ °C to $T_f = 25.6$ °C corresponds to an unfolding and loss of helicity of just 4%.

Table 1
Helical content (f_{H}) and protonation degree of PGA in dependence of pD (at $T = 25$ °C).

Degree of protonation	pD	θ_{222} [deg cm ⁻² dmol ⁻¹]	f_{H} [%]
0%	8.3	4.81E+05	0
10%	7.6	3.86E+05	0
20%	7.2	3.67E+05	0
30%	6.9	2.22E+05	0
40%	6.7	2.76E+03	0
50%	6.4	-1.71E+05	4.4
60%	6.3	-5.88E+05	14.9
65%	6.2	-1.75E+06	44.4
70%	5.9	-2.56E+06	64.8
75%	5.7	-3.66E+06	92.8
80%	5.2	-3.75E+06	94.9
90%	4.8	-4.09E+06	103.5
100%	4.1	(-3.59E+06)	(91)

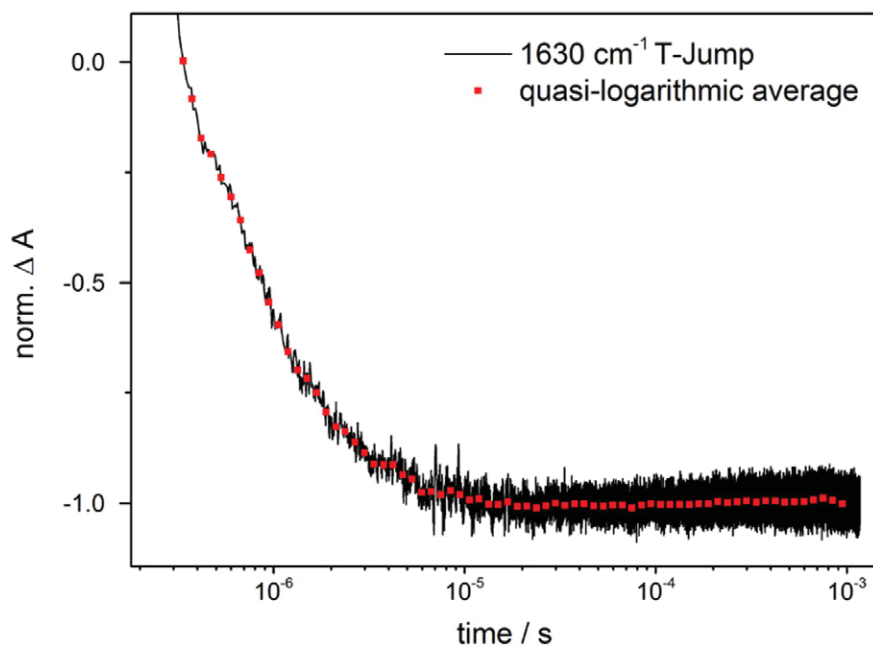


Fig. 3. Quasi-logarithmic averaging. A comparison of the raw data with previous solvent subtraction is shown before and after a quasi-logarithmic averaging with $N = 20$ points per decade. A significant reduction of the noise amplitude is achieved and the data points at early time scale are not underrepresented in the fit procedure.

3.2. Kinetic studies and data evaluation

For a reliable interpretation of the kinetic data, the choice of an appropriate fit function is very important. Relaxation dynamics of PGA have previously been described with mono-exponential [7,10,23], bi-exponential [5] or stretched exponential [9] functions. We applied all these functions to our T-jump and pH-jump kinetic data in order to

evaluate the best fit (Fig. 5). Compared to our previous PGA measurements [10] where we applied a mono-exponential fit function, we now have a much better data quality in particular due to a significantly reduced signal noise and the accessibility of an extended fit interval including time points below 500 ns.

Several efficient improvements were made in our spectrometer setup. One is the replacement of the previously used lead salt diodes

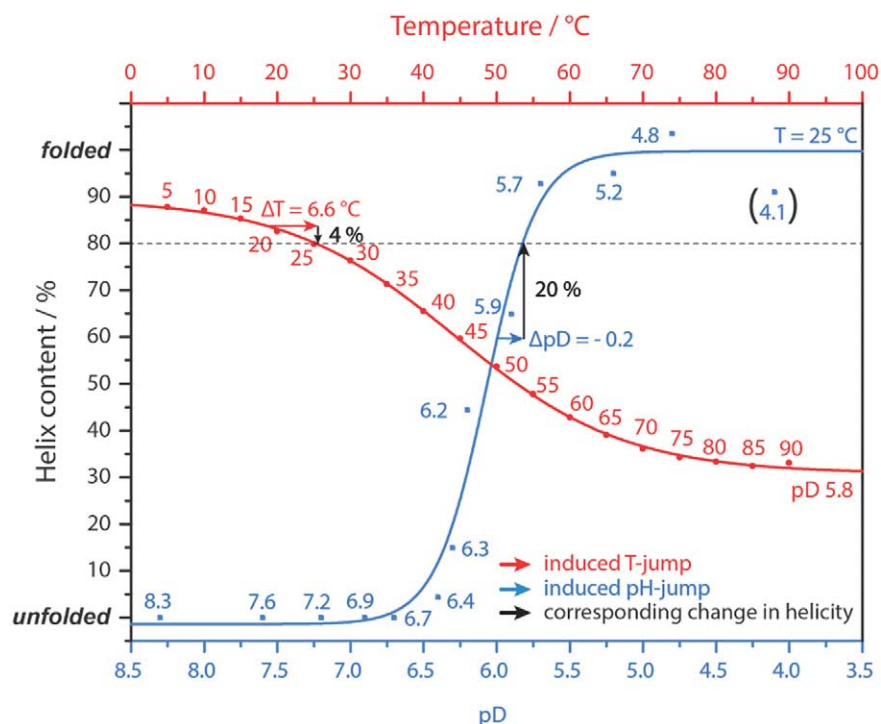


Fig. 4. Temperature- and pD-dependent helix content of PGA. The thermal unfolding process was monitored from 5 °C to 90 °C at pD 5.8 (red curve). Fitting the data yields a transition temperature of $T_m = 44$ °C. The applied T-jump corresponds to a change in helix content of about 4%. The titration of PGA was carried out at 25 °C (blue curve). An increase in helix content of 20% corresponds to a pH-jump of $\Delta\text{pD} = -0.2$. The dotted line indicates that both perturbation experiments proceed to the same final PGA conformation with 80% helix content.

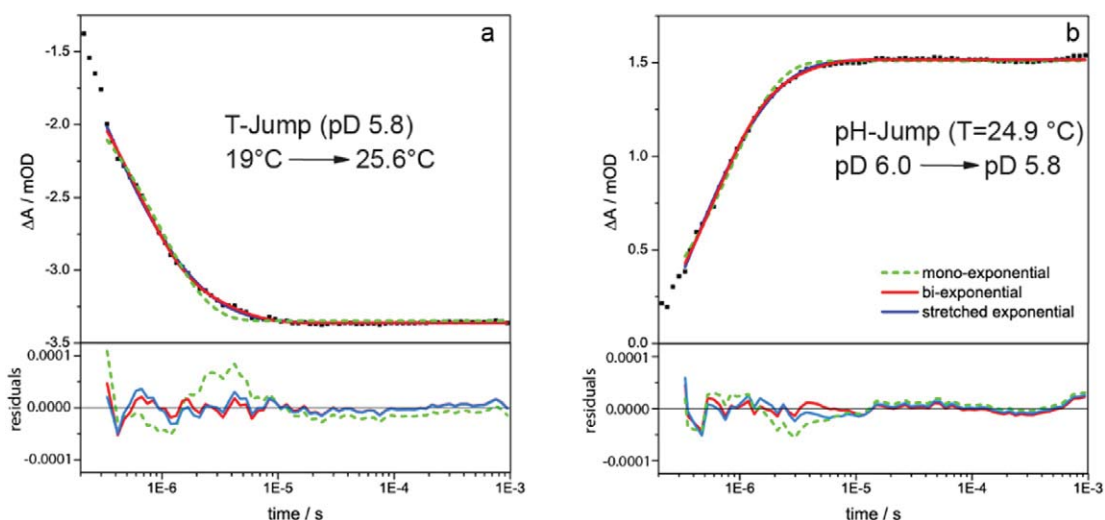


Fig. 5. Relaxation dynamics of PGA probed at 1630 cm^{-1} after laser-excited perturbation. The transients of PGA were fitted by a mono-exponential (dashed green line), a bi-exponential (red line) and a stretched exponential function (blue line). Residuals of the fits are shown in the lower panels. a) T-jump and unfolding b) pH-jump and folding of PGA to the helical content of $\sim 80\%$ at pD 5.8 and $T \approx 25^\circ\text{C}$.

[24] by quantum cascade lasers [20]. The power of the emission spectrum is increased by a factor of 100–1000 resulting in a significantly better signal-to-noise of the data. In addition, QCLs are characterized by a continuous tunability of the IR modes in contrast to lead salt diodes which exhibited mode hopping and thereby restricting the accessibility of probe wavelengths. Furthermore, for excitation of the T-jump, the Nd:YAG/Raman shifter combination was replaced by a Ho:YAG laser. As has been shown recently, the Ho-YAG laser's fundamental wavelength can be used to excite the water overtone vibration directly without a Raman shifter [25]. The Ho:YAG laser provides a much better shot-to-shot stability and beam profile quality compared to the Raman-shifted Nd:YAG laser. The non-linear processes in Raman shifting result in a non-uniform beam profile with hot spots and large shot-to-shot fluctuations. Thus the use of a Ho:YAG laser contributes significantly to improve the T-jump data since the T-jump magnitude is better defined and also the adjustment of the pump pulse with the probe beam can be performed more accurately. Due to the reduced distortions caused by the excitation, we could extend the evaluable data and thus the fit interval to earlier data points compared to [10], but also to later data points due to a different treatment of the water dynamics. In [10] we included the water cooling in a bi-exponential model to decompose the contributions from the water and the peptide, each represented by a mono-exponential function. This is a decent approximation only for early time scales since the water dynamics becomes strongly non-exponential on longer time scales [26]. Previously we used a fit-interval restricted up to $200\ \mu\text{s}$ [10]. Here, we subtracted the water dynamics by separate measurements and thus the water dynamics had not to be implemented in the fit model as before. A better data quality could also be achieved by the quasi-logarithmic averaging procedure as describe above.

Fig. 5 shows the relaxation dynamics of PGA probed at 1630 cm^{-1} after the T-jump/pH-jump and the evaluation of the transients with various fit functions. Fig. 5a reveals that the decrease of α -helical content measured at 1630 cm^{-1} is only poorly described by a mono-exponential function (dashed green line). This becomes also obvious in the corresponding residuals of the fits shown in the lower panels. In contrast, bi-exponential (red line) or stretched exponential (blue line) functions fit the experimental data well. However, for the stretched exponential function the stretching factor β strongly varies upon the evaluated fit-interval (e.g. $\beta = 0.44$ for 340 ns – 1 ms and $\beta = 0.31$ for 500 ns – 1 ms) and adapts values far below 1 indicating a heavily stretched function. In contrast, the bi-exponential function is very robust and shows only marginal changes in the resulting relaxation times if the fit-interval is

varied. A similar behavior is observed for the pH-jump relaxation data (Fig. 5b). We concluded that a bi-exponential function is best-suited to describe our data. The relaxation times obtained for the T-jump and pH-jump measurements are given below.

3.3. T-jump induced conformational dynamics

The T-jump experiment was performed in the amide I' region at 1630 cm^{-1} reflecting the changes in the α -helical structure of PGA under the influence of the elevated temperature from 19°C to 25.6°C . The pD was adapted to 5.8, the final value in the pH-jump experiment. Under those conditions unfolding of PGA remains fully reversible and shows no signs of aggregation confirmed by FTIR-measurements (data not shown). The temperature-dependent FTIR measurements show an absorbance change $\Delta A \sim 3.6\text{ mOD}$ at 1630 cm^{-1} upon temperature increase from 18.8°C to 25.5°C correlating well with $\Delta A \sim 3.4\text{ mOD}$ in our T-jump measurements (Fig. 5a). Thus the FTIR-measurements confirm our estimate of the T-jump magnitude. The applied T-jump induced a relatively small change in helicity decreasing from $\sim 84\%$ to 80% α -helical conformation (Fig. 4). Fig. 5a presents the relaxation kinetics for the decrease in helical content. The bi-exponential fit function yields one fast component $\tau_1 = 548\text{ ns}$ with an amplitude of 1.71 mOD and a slow component $\tau_2 = 2.84\ \mu\text{s}$ with an amplitude of 0.43 mOD . We could now resolve an additional kinetic step compared to our previous T-jump studies on PGA [10] that were performed using lead salt diodes as IR source yielding a much poorer signal-to-noise as compared to the now used QCL.

3.4. pH-jump induced conformational dynamics

The CD-calibration curve shown in Fig. 4 indicates the steepest transition in the pD range between 6.5 and 5.5. Thus the initial pD value was chosen to be at pD 6.0. Despite the relatively small pH-jump of -0.2 , the amplitude of the folding signal was high enough to monitor the growth of the α -helical content. The temperature was adjusted to $T = 23.9^\circ\text{C}$ since the final sample temperature was elevated by $\sim 1^\circ\text{C}$ due to the additional temperature jump which arises from the UV excitation beam as described in Section 2.3.2. Thus the pH-experiment was performed with a final temperature of $T_f = 24.9^\circ\text{C}$. The bi-exponential fit function yielded the time constants $\tau_1 = 629\text{ ns}$ with an amplitude of -1.91 mOD and $\tau_2 = 3.00\ \mu\text{s}$ with an amplitude of -0.2 mOD . The pH-jump induced an increase in helicity from $\sim 60\%$ to $\sim 80\%$ (Fig. 4). The helix unfolding due to the intrinsic T-jump is marginal and was neglected in

the quantification of the helicity. The pH-jump experiment was not carried out in a double beam geometry (as it was the case for the T-jump experiment) and the estimated pH-jump amplitude is an average. The used α NBA concentration is relatively high and thus the strong absorbance at 266 nm will cause an inhomogeneity along the beam path since the pump beam intensity at the back face of the sample is significantly less than that at the front face. The beam inhomogeneity along the optical path contributes to the deviations from a mono-exponential behavior observed here, however not to a sufficient extent.

3.5. Comparison of both perturbation techniques

PGA is a well suited peptide model system to gain insights into the process of α -helix folding, a multi-step mechanism involving helix nucleation, hydrogen bond formation and helix propagation. The peptide is particularly challenging for pH-jump and T-jump measurements since both, pH and temperature are parameters that control its conformation, but not in an independent manner. The pH determines the protonation degree of the PGA side-chains and in turn the degree in helicity. Acidic pH is necessary for PGA helix folding and it can be reversibly unfolded and refolded by temperature in a certain pH range, but there are also pH/temperature conditions where it irreversibly aggregates [10,27]. Previous pH-jump studies of PGA revealed that helix nucleation occurs in less than 40 ns and that the folding kinetics depend on the initial fraction of helical residues [5] and peptide length/number of residues [7]. Also T-jump studies have been performed and relaxation dynamics were observed with IR [9,10] and CD probing [11,23]. The absolute values and numbers of observed relaxation times depend on the experimental conditions used and it becomes obvious that PGA helix formation is a process with several kinetic steps.

In the current study, we performed T-jump and pH-jump measurements on the same PGA sample and thus could directly compare the two perturbation techniques. We designed the experiments in that way that the same pD and temperature, and thus a comparable final conformation is captured at the new equilibrium. We assume that we operate under experimental conditions where the PGA conformation is only determined by the two parameters temperature and pH. One should note that the two excitation paths, one changing the temperature whereas the other changes the proton concentration, are not completely independent. For example, the proton concentration depends on the pK_a and the pK_a is temperature-dependent. Thus a T-jump might result in a pH change. However, in the case of glutamic acid, the temperature dependence of the pK_a is very weak [28,29] so that we assume to have a negligible T-jump induced protonation change in our PGA studies. The starting conformations were different, but both had a significant initial helix fraction, ~84% for the T-jump experiment and ~60% for the pH-jump experiment. The change in helicity was much less upon T-jump unfolding (4%) than pH-jump folding (20%) what can be explained by the strong pH-dependence of this specific homopolypeptide with solely titratable side-chains. The observed transients were best described by a bi-exponential fit for both perturbation experiments. In comparison to our previous PGA T-jump study [10], we could now resolve an additional kinetic step due to the significant improvements in our spectrometer setup, as described in Section 3.2, resulting in a much higher data quality. The replacement of lead salt diodes by quantum cascade lasers was a crucial contribution. Although the helicity change is significantly larger in the pH-jump than in the T-jump experiment, the time constants are only marginally slower and might be regarded as similar within the experimental error.

As shown in Fig. 5, a bi-exponential function fits our data very well. The deviations from a mono-exponential behavior which the data show for both, T-jump and pH-jump measurements, are relatively minor (also indicated by the relative amplitudes of the time constants given in Sections 3.3. and 3.4) and may have a number of reasons. Some of these are experimental, e.g. the inhomogeneity of the pH-jump as mentioned in Sections 3.4, or the inhomogeneous molecular weight of the

polypeptide sample. However, non-exponential helix-coil relaxation has been observed before [9] and is in fact expected for this process, since helical polypeptides do not adopt a homogeneous state, but rather a very broad and dynamic distribution of states with more or less helical content, which could easily have slightly different helix relaxation kinetics. Also, helical unfolding of 4% of a peptide with 136 residues means that five residues lose helical structure (on average), which most likely occurs consecutively, i.e. in a multi-step behavior, necessarily yielding small deviations from exponential behavior even if each step has the same rate constant. Residue reorientation upon helix propagation might also contribute to a non-exponential relaxation.

Since we have partially folded helices before and after the perturbation in both of our experiments and we never reach a completely unfolded state, we cannot observe any helix nucleation step. Our applied T-jumps and pH-jumps are relatively small and induce melting or propagation of the helix by a limited number of residues. The initial and the jump conditions were chosen to achieve the same final state in both perturbation experiments. Thus, by applying the combination of laser-excited T-jump and pH-jump perturbation methods, we observe helix folding and unfolding of PGA under comparable conditions. The observed time constants are similar and indicate that helix folding and unfolding proceed with the same molecular mechanism.

4. Conclusion

We have built a quantum cascade laser-based IR-spectrometer to study folding mechanisms with perturbation techniques. Pulsed lasers are used to induce a nanosecond pH-jump or T-jump, and to monitor the relaxation dynamics of the biomolecule to the new equilibrium. We applied both perturbation methods to study the conformational dynamics of PGA and compared pH-induced folding and T-jump induced unfolding by the quantitatively determined change in helicity. Temperature and pH are the main determinants for the conformation of PGA. Small perturbations have been applied ($\Delta pD = -0.2$ °C, $\Delta T = 6.6$ °C) and relaxation dynamics to the same final degree in helicity were monitored upon folding respectively unfolding. In both experiments the observed kinetics were similar thus independent from the perturbation technique indicating the same mechanism for helix folding and unfolding. Probing non-equilibrium dynamics is useful, in particular when the protein under study folds in a multi-step process with a variety of intermediate states.

Acknowledgement

We gratefully acknowledge financial support by the Deutsche Forschungsgemeinschaft (SFB 969 and SFB 1214) and the Center of Applied Photonics Konstanz (CAP 13).

References

- [1] R.H. Callender, R.B. Dyer, R. Gilmanshin, W.H. Woodruff, Fast events in protein folding: the time evolution of primary processes, *Annu. Rev. Phys. Chem.* 49 (1998) 173–202.
- [2] W.A. Eaton, V. Munoz, S.J. Hagen, G.S. Jas, L.J. Lapidus, E.R. Henry, J. Hofrichter, Fast kinetics and mechanisms in protein folding, *Annu. Rev. Biophys. Biomol. Struct.* 29 (2000) 327–359.
- [3] K. Hauser, C. Krejtschi, R. Huang, L. Wu, T.A. Keiderling, Site-specific relaxation kinetics of a tryptophan zipper hairpin peptide using temperature-jump IR spectroscopy and isotopic labeling, *J. Am. Chem. Soc.* 130 (2008) 2984–2992.
- [4] A. Popp, L. Wu, T.A. Keiderling, K. Hauser, Effect of hydrophobic interactions on the folding mechanism of β -hairpins, *J. Phys. Chem. B* 118 (2014) 14234–14242.
- [5] T.P. Causgrove, R.B. Dyer, Nonequilibrium protein folding dynamics: laser-induced pH-jump studies of the helix-coil transition, *Chem. Phys.* 323 (2006) 2–10.
- [6] M.L. Donten, P. Hamm, pH-jump overshooting, *J. Phys. Chem. Lett.* 2 (2011) 1607–1611.
- [7] M.L. Donten, P. Hamm, pH-jump induced α -helix folding of poly-L-glutamic acid, *Chem. Phys.* 422 (2013) 124–130.
- [8] M.L. Donten, S. Hassan, A. Popp, J. Halter, K. Hauser, P. Hamm, pH-jump induced leucine zipper folding beyond the diffusion limit, *J. Phys. Chem. B* 119 (2015) 1425–1432.

- [9] E.A. Gooding, S. Sharma, S.A. Petty, E.A. Fouts, C.J. Palmer, B.E. Nolan, M. Volk, pH-Dependent helix folding dynamics of poly-glutamic acid, *Chem. Phys.* 422 (2013) 115–123.
- [10] C. Krejtschi, K. Hauser, Stability and folding dynamics of polyglutamic acid, *Eur. Biophys. J.* 40 (2011) 673–685.
- [11] L. Mendonça, A. Steinbacher, R. Bouganne, F. Hache, Comparative study of the folding/unfolding dynamics of poly(glutamic acid) in light and heavy water, *J. Phys. Chem. B* 118 (2014) 5350–5356.
- [12] D.T. Clarke, A.J. Doig, B.J. Stapley, G.R. Jones, The α -helix folds on the millisecond time scale, *Proc. Natl. Acad. Sci. U. S. A.* 96 (1999) 7232–7237.
- [13] M.J. Gregory, M. Anderson, T.P. Causgrove, Measurement of energy barriers to conformational change in poly-L-glutamic acid by temperature-derivative spectroscopy, *Chem. Phys.* 420 (2013) 1–6.
- [14] T. Kimura, S. Takahashi, S. Akiyama, T. Uzawa, K. Ishimori, I. Morishima, Direct observation of the multistep helix formation of poly-L-glutamic acids, *J. Am. Chem. Soc.* 124 (2002) 11596–11597.
- [15] C.A. Rohl, R.L. Baldwin, Comparison of NH exchange and circular dichroism as techniques for measuring the parameters of the helix – coil transition in peptides, *Biochemistry* 36 (1997) 8435–8442.
- [16] S. Abbuzzetti, C. Viappiani, J.R. Small, L.J. Libertini, E.W. Small, Kinetics of local helix formation in poly-L-glutamic acid studied by time-resolved photoacoustics: neutralization reactions of carboxylates in aqueous solutions and their relevance to the problem of protein folding, *Biophys. J.* 79 (2000) 2714–2721.
- [17] J.M. Finke, P.A. Jennings, J.C. Lee, J.N. Onuchic, J.R. Winkler, Equilibrium unfolding of the poly(glutamic acid)₂₀ helix, *Biopolymers* 86 (2007) 193–211.
- [18] A.K. Covington, Use of the glass electrode in deuterium oxide and the relation between the standardized pD (p_{aD}) scale and the operational pH in heavy water, *Anal. Chem.* 40 (1968) 700–706.
- [19] P. Luo, R.L. Baldwin, Mechanism of helix induction by trifluoroethanol: a framework for extrapolating the helix-forming properties of peptides from trifluoroethanol/water mixtures back to water, *Biochemistry* 36 (1997) 8413–8421.
- [20] A. Popp, D. Scheerer, H. Chi, T.A. Keiderling, K. Hauser, Site-specific dynamics of β -sheet peptides with ^DPro-Gly turns probed by laser-excited temperature-jump infrared spectroscopy, *ChemPhysChem* 17 (2016) 1273–1280.
- [21] M.V. George, J.C. Scaiano, Photochemistry of *o*-nitrobenzaldehyde and related studies, *J. Phys. Chem.* 84 (1980) 492–495.
- [22] J.Y. Cassim, J.T. Yang, Effect of molecular aggregation on circular dichroism and optical rotatory dispersion of helical poly-L-glutamic acid in solution, *Biochem. Biophys. Res. Commun.* 26 (1967) 58–64.
- [23] L. Mendonça, F. Hache, Nanosecond T-jump experiment in poly(glutamic acid): a circular dichroism study, *Int. J. Mol. Sci.* 13 (2012) 2239.
- [24] C. Krejtschi, R. Huang, T.A. Keiderling, K. Hauser, Time-resolved temperature-jump infrared spectroscopy of peptides with well-defined secondary structure: a Trpzip β -hairpin variant as an example, *Vib. Spectrosc.* 48 (2008) 1–7.
- [25] D. Li, Y. Li, H. Li, X. Wu, Q. Yu, Y. Weng, A Q-switched Ho:YAG laser assisted nanosecond time-resolved T-jump transient mid-IR absorbance spectroscopy with high sensitivity, *Rev. Sci. Instrum.* 86 (2015) 053105.
- [26] A.P. Ramajo, S.A. Petty, M. Volk, Fast folding dynamics of α -helical peptides – effect of solvent additives and pH, *Chem. Phys.* 323 (2006) 11–23.
- [27] A. Hernik, W. Pulawski, B. Fedorczyk, D. Tymecka, A. Misicka, S. Filipek, W. Dzwolak, Amyloidogenic properties of short α -L-glutamic acid oligomers, *Langmuir* 31 (2015) 10500–10507.
- [28] H. Nagai, K. Kuwabara, G. Carta, Temperature dependence of the dissociation constants of several amino acids, *J. Chem. Eng. Data* 53 (2008) 619–627.
- [29] R. Wolfenden, C. Lewis Jr., Y. Yuan, C. Carter Jr., Temperature dependence of amino acid hydrophobicities, *Proc. Natl. Acad. Sci. U. S. A.* 112 (2015) 7484–7488.